

Synthesis, molecular and crystal structure analysis of 2-bromo-4-chloro-6-[[4-(3-methyl-3-phenyl-cyclobutyl)-thiazol-2-yl]-hydrazonomethyl]-phenol by experimental methods and theoretical calculations

Feyizan Güntepe^{a,*}, Hanife Saraçoğlu^b, Nezihe Çalışkan^c, Çiğdem Yüksektepe^d, Alaaddin Cukurovali^e

^a Department of Physics, Faculty of Arts and Sciences, Ondokuz Mayıs University, Samsun, Turkey

^b Department of Physics Education, Faculty of Education, Ondokuz Mayıs University, Samsun, Turkey

^c Department of Physics, Faculty of Sciences, Gazi University, Ankara, Turkey

^d Department of Physics, Faculty of Science, Cankiri Karatekin University, Cankiri, Turkey

^e Department of Chemistry, Faculty of Science, Firat University, Elazığ, Turkey

H I G H L I G H T S

- We investigate molecular and crystal structure of the new hydrazone derivative.
- Crystal structure is stabilized by N–H···O, O–H···O and C–H···O type hydrogen bonds.
- The calculated frequencies for $\nu_{\text{str}}(\text{O–H})$ and $\nu_{\text{str}}(\text{N–H})$ higher the experimental ones.

A R T I C L E I N F O

Article history:

Received 17 September 2011

Received in revised form 1 May 2012

Accepted 1 May 2012

Available online 14 May 2012

Keywords:

Hydrazone

Crystal structure

IR spectroscopy

DFT calculation

A B S T R A C T

A novel hydrazone derivative 2-bromo-4-chloro-6-[[4-(3-methyl-3-phenyl-cyclobutyl)-thiazol-2-yl]-hydrazonomethyl]-phenol was synthesized and characterized by IR, UV–Vis spectroscopy and X-ray single crystal diffraction. The compound crystallizes in monoclinic space group $P2_1/c$ with $a = 8.0862(3) \text{ \AA}$, $b = 7.6168(1) \text{ \AA}$, $c = 37.3168(12) \text{ \AA}$ and $\beta = 91.186(1)^\circ$. In addition, the molecular geometry and vibrational frequencies of the title compound in ground state have been calculated by using density functional theory (DFT) at B3LYP level with 6-31G and 6-31G(d,p) basis sets. The geometrical parameters of the title compound obtained from XRD studies are in good agreement with the calculated values. The analysis of IR spectrum supported by DFT calculations was particularly devoted to the manifestations of hydrogen bonding in the $\nu_{\text{str}}(\text{N–H})$ and $\nu_{\text{str}}(\text{O–H})$ vibrations. To determine the conformational flexibility for a selected torsion angle $\tau(\text{C6–C1–C7–N1})$ one-dimensional potential energy scan was performed using AM1 in the full range of 0–360° increasing of 10°. UV–Vis absorption spectrum of the compound has been compared to theoretical spectrum (vertical excitations) computed by time dependent density functional theory (TD-DFT). Besides frontier molecular orbitals and molecular electrostatic potential map analysis were investigated by theoretical calculations.

© 2012 Elsevier B.V. All rights reserved.

1. Introduction

Hydrazones are an important class of compounds due to their diverse applications. Hydrazones and their metal complexes possess pronounced biological and pharmaceutical activities as antitumor [1–4], antimicrobial [5], antituberculosis [6] and antimalarial agents [7]. Hydrazones play an important role in improving the antitumor selectivity and toxicity profile of antitumor agents by

forming drug carrier system employing suitable carrier proteins [8]. They are also employed as extracting agents in spectrophotometric determination of some ions [9–11] and spectrophotometric determination of some species in pharmaceutical formulations [12], as well as waste water treatment [13]. Metal complex of hydrazones have found applications in various chemical processes like non-linear optics and sensors [14] and have been used in the separation and concentration of palladium and platinum in road dust [15]. Hydrazones have found wide applications in synthetic chemistry [16], to be used as indicators. Hydrazones have been utilized for the determination of carbonyl compounds [17,18]. The

* Corresponding author. Fax: +90 362 4576081.

E-mail address: feyizanguntepe@gmail.com (F. Güntepe).

hydrazones have been used for different purposes such as herbicides, insecticides, nematocides and plant growth regulators [19]. The hydrazones are also important for their use as plasticizers and stabilizers for polymers [20], polymerization initiators and antioxidant [21].

The title compound 2-bromo-4-chloro-6-[[4-(3-methyl-3-phenyl-cyclobutyl)-thiazol-2-yl]-hydrazonomethyl]-phenol is a kind of hydrazone derivatives. Beside of its possible pharmacological relevance this molecule is also an interesting model for studies vibrational spectrum in hydrogen bonding system. Vibrational spectrum provides the most commonly used criteria for the presence and properties of hydrogen bonds. The most significant spectral changes resulting from H-bond formation occur in the IR spectrum in particular in the region of X–H stretching bands. These are the decrease in frequency in the N–H stretching mode, increase of its intensity, broadening of the bands and appearance of a complex fine structure [22]. The mechanisms of these phenomena are subject of many theoretical studies. On the other hand an alternative computational methods have long been carried out for equilibrium structure properties of molecular system such as geometry and vibrational frequency. Computational methods are at present widely used for simulating IR spectrum [1]. Such simulations are indispensable tools to perform normal mode analysis so that modern vibrational spectroscopy is unimaginable without involving them. In this paper, we present the result of the detailed investigation of synthesis and structural characterization of title compound using XRD, IR and UV–Vis spectroscopy and quantum chemical methods. The geometric parameters and vibrational frequencies of the title compound in ground state were calculated DFT/B3LYP method with 6-31G and 6-31G(d,p) basis sets. The aim of the study is an analysis and discussion of results for one representative member of this hydrazone family. These discussions are valuable for providing insight into molecular structure and chemical behavior.

2. Experimental

2.1. General remarks

Melting point was determined by Gallencamp melting point apparatus. FT-IR spectrum was recorded on KBr pellet with a ATI Unicam-Mattson 1000 FT-infrared spectrometer 4000–400 cm^{-1} range. The UV spectrum of the compound was performed on a Shimadzu UV-1700 spectrometer in CHCl_3 solvent. All reagents were commercially obtained and used without any further purification.

2.2. Synthesis

The title compound was synthesized as shown in Scheme 1 by the following procedure. To a stirred solution of 3-bromo-5-chloro salicylaldehyde (10 mmol) in 30 mL of ethanol, thiosemicarbazide (10 mmol) was added portions. Subsequently, a solution of phenacyl chloride (10 mmol) in 20 mL of ethanol was added dropwise. After the addition of the α -haloketone, the temperature was kept

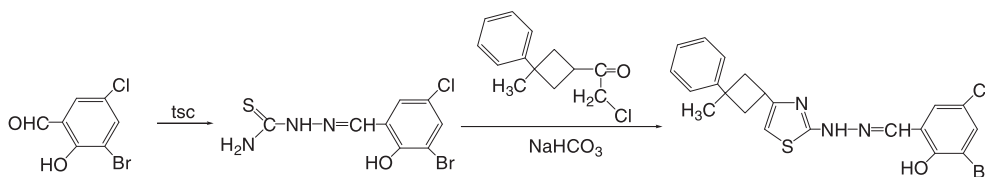
Table 1
Crystallographic data for title compound.

Empirical formula	$\text{C}_{21}\text{H}_{19}\text{BrClN}_3\text{OS}\cdot\text{H}_2\text{O}$
Molecular weight	476.81
Temperature (K)	296
Wavelength (Å)	0.71073 Mo $\text{K}\alpha$ radiation
Crystal system	Monoclinic
Space group	$\text{P2}_1/\text{c}$
Unit cell dimensions (Å, °)	$a = 8.0862(3)$ $b = 7.6168(1)$ $c = 37.3168(12)$ $\alpha = 90$ $\beta = 91.186(1)$ $\gamma = 90$
Volume (Å ³)	2297.89(12)
Z	4
Calculated density (mg m^{-3})	2.757
μ (mm^{-1})	2.02
Absorption correction	Integration (X-RED32)
$T_{\text{min}}, T_{\text{max}}$	0.2210, 0.4396
Crystal size (mm)	$0.60 \times 0.46 \times 0.18$
Diffractometer/measurement	STOE IPDS 2/rotation (ω scan)
Index ranges (h, k, l)	$h = -9 \rightarrow 9, k = -9 \rightarrow 9, l = -45 \rightarrow 45$
Θ Range (°)	2.2–25.6
Reflections collected	21,535
Independent reflections	4326
Observed reflections [$I > 2\sigma(I)$]	3381
R_{int}	0.054
Refinement method	Full-matrix least-squares on F^2
Goodness-of-fit on F^2	1.04
R ($I > 2\sigma$)	0.042
wR ($I > 2\sigma$)	0.110
$\Delta\rho_{\text{max}}, \Delta\rho_{\text{min}}$	0.36, –0.51
Extinction coefficient	0.0008(4)
CCDC	777381

at 323–328 K for 2 h more. After cooling to the room temperature the solution was then made alkaline with an aqueous solution of NH_3 (5%), and a light olive green precipitate separated. The precipitate was filtered off, washed with aqueous NH_3 solution several times and dried in air. Suitable single crystals for crystal structure determination were obtained by slow evaporation of its ethanol solution. Yield: 77%, melting point: 449 K.

2.3. X-ray crystal structure determination

Data collection was carried out on a Stoe-IPDS-2 diffractometer equipped with a graphite monochromated Mo $\text{K}\alpha$ radiation ($\lambda = 0.71073$ Å) at 293 K. The structure was solved by direct methods using SHELXS-97 [23] implemented in the WinGX software system [24] and refined by full-matrix least-squares procedure using SHELXL-97 [25]. All non-hydrogen atoms were easily found from the difference Fourier map and refined anisotropically. All hydrogen atoms were included using a riding model and refined isotropically with $\text{C–H} = 0.93\text{–}0.97$ Å and $\text{N–H} = 0.86$ Å. $U_{\text{iso}}(\text{H}) = 1.2U_{\text{eq}}(\text{C}, \text{N})$, $U_{\text{iso}}(\text{H}) = 1.5U_{\text{eq}}$ (for methyl group). Data collection, X-AREA [26]; cell refinement X-AREA; data reduction, X-RED32 [26] The molecular structure plots were prepared by using the



Scheme 1. The synthesis pathway of the title compound.

ORTEP III [27]. Crystallographic data, details of the data collection and structure refinements are listed in Table 1.

2.4. Computational methods

All the calculations are performed for the title compound by using Gaussian 03 program package on a personal computer [28]. The molecular structure of the title compound in the ground state (in vacuo) was optimized using DFT/B3LYP [29,30] method with following standard basis sets: 6-31G, valance double zeta functions and 6-31G(d,p), valance double zeta plus polarization functions of d and p type. For modeling the initial guess of title compound was obtained from the X-ray refinement data. The harmonic vibrational frequencies analysis was performed at the same level of theory. No scale factor was used in the calculated frequencies. The molecular electrostatic potential map and frontier molecular orbital surfaces are visualized by GausView Molecular Visualization program [31].

3. Result and discussion

3.1. Crystallographic results

The title compound which is shown in Fig. 1 as an Ortep III view, crystallizes in monoclinic space group $P2_1/c$ with four molecules in the unit cell. The asymmetric unit in the crystal structure contains only one molecule with a crystalline water.

The title molecule is composed of a central thiazole ring with 2-bromo-4-chloro-phenol group connected to the 2-position of the ring via hydrazone group and 3-methyl-3-phenyl-cyclobutyl in the 4-position. The thiazole ring A (S1/C10/C9/N3/C8), phenol ring B (C1–C6) and phenyl ring C (C16–C21) are each approximately planar. The dihedral angle between these rings are $1.6(2)^\circ$, $77.6(2)^\circ$ and $78.8(2)^\circ$ for A/B, A/C and B/C respectively. The steric interaction between the substituent groups on the cyclobutane ring D (C11–C14) means that this ring deviates significantly from planarity. In this case the C14/C13/C12 plane forms a dihedral angle of $23.3(2)^\circ$ with the C12/C11/C14 plane in cyclobutane ring. Similar puckering of cyclobutane ring has been reported $23.5(2)^\circ$ [32] and $24.09(12)^\circ$ [33]. In thiazole ring there are two different C–N bond distances, viz. C8=N3 and C9–N3. The C8=N3 double bond length is $1.307(3)$ Å and C9–N3 single bond is $1.381(4)$ Å. The C9=C10 bond length is $1.343(4)$ Å, characterizing a C=C double bond. The S1–C8 and S1–C10 bond distances are shorter than the accepted value for an S–Csp² single bond with 1.76 Å [34] resulting from the conjugation of the electrons of atom S1 with atoms C8 and C10 [35]. The experimental N–N bond length of

hydrazone is reported as 1.449 Å [36] and electron diffraction N–N bond length of tetramethylhydrazone is reported at 1.401 Å [37] while for the title compound the N1–N2 bond length of hydrazone (C7=N1–N2) fragment is $1.367(3)$ Å which is somewhere between the length of Nsp²–Nsp² single bond (1.401 Å) [38] and N=N double bond (1.25 Å) [1]. The X-ray studies have showed that the –OH group is in an ortho-position to the hydrazone linkage which enable O1–H1...N1 intramolecular hydrogen bond producing a graph set motif of S(6) [39]. In the crystal lattice the hydrogen bonds established via water molecule. The atom O(2) of water at (x,y,z) acts as a bifurcated hydrogen bond donor to atoms N(3) at (x,y,z) and O(1) at (1–x,2–y,–z), with inversion symmetry, via H2WA and H2WB respectively. Besides of this the atom O(2) of water at (x,y,z) acts as a bifurcated hydrogen bond acceptor to atoms N(2) and C(7) at (1–x,1–y,–z). Therefore molecules are packed by intermolecular hydrogen bonds in zigzag arrangement parallel to c axis in the crystal structure as seen from Fig. 2. The details of hydrogen bonds are given in Table 2.

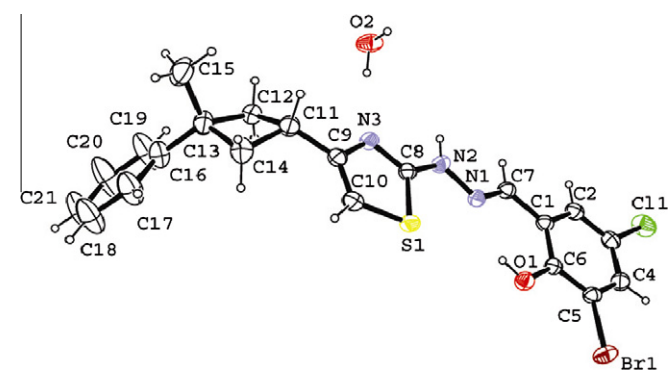


Fig. 1. ORTEP drawing of the basic crystallographic unit of the title compound, showing the atom-numbering scheme. Displacement ellipsoids are drawn at the 50% probability level and all H atoms are shown as small spheres of arbitrary radii.

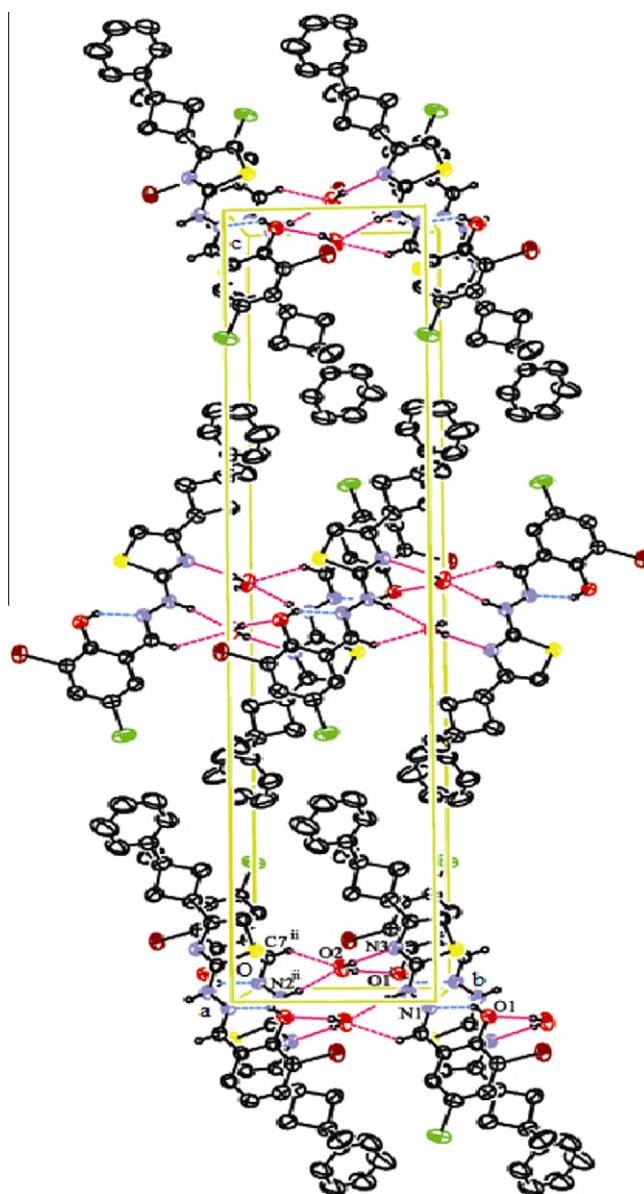


Fig. 2. A partial packing diagram of the title compound, hydrogen bonding interactions have been shown as broken lines.

Table 2
Hydrogen bonding geometries for the title compound.

D—H...A	D—H (Å)	H...A (Å)	D...A (Å)	D—H...A (°)
O1—H1...N1	0.82	1.90	2.620(3)	147
O2—H2WA...N3	0.82(3)	2.07(3)	2.840(4)	157(3)
O2—H2WB...O1 ⁱ	0.84(3)	2.14(3)	2.953(4)	163(3)
N2—H2A...O2 ⁱⁱ	0.86	1.98	2.790(3)	158
C7—H7...O2 ⁱⁱ	0.93	2.44	3.206(4)	140

Symmetry code: (i) 1 - x, 2 - y, -z; (ii) 1 - x, 1 - y, -z.

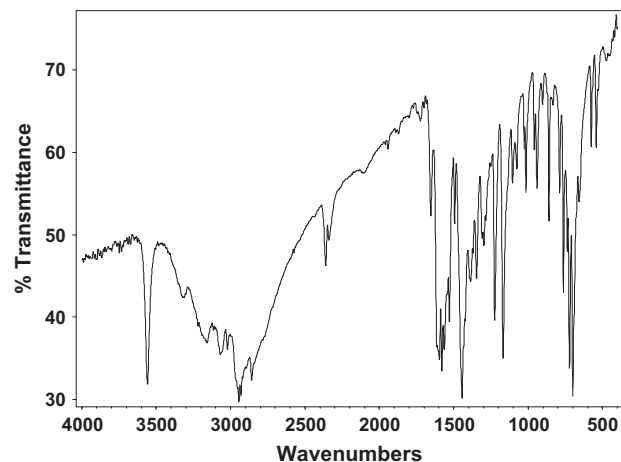
Table 3
Selected experimental and optimized geometric parameters of the title compound.

Parameter	Experimental	DFT/B3LYP	
		6-31G	6-31G(d,p)
<i>Bond lengths (Å)</i>			
N1—C7	1.284(4)	1.305	1.295
N1—N2	1.367(3)	1.363	1.350
N2—C8	1.343(4)	1.363	1.367
N3—C8	1.307(3)	1.317	1.311
N3—C9	1.381(4)	1.406	1.389
C9—C10	1.343(4)	1.360	1.362
S1—C8	1.728(3)	1.817	1.755
S1—C10	1.725(3)	1.818	1.753
C11—C12	1.540(4)	1.568	1.559
C12—C13	1.546(5)	1.573	1.564
C13—C14	1.549(5)	1.575	1.565
C14—C11	1.536(5)	1.557	1.550
O1—C6	1.350(3)	1.339	1.340
C9—C11	1.488(4)	1.495	1.496
C16—C13	1.512(5)	1.519	1.517
C16—C17	1.354(6)	1.405	1.401
C18—C21	1.320(8)	1.399	1.395
C17—C18	1.381(7)	1.399	1.395
C16—C19	1.352(6)	1.405	1.401
C19—C20	1.389(6)	1.399	1.395
C20—C21	1.312(7)	1.399	1.395
RMSE ^a		0.045	0.032
Max. difference ^a		0.093	0.083
<i>Bond angles (°)</i>			
C10—S1—C8	88.32(14)	86.32	87.85
C9—N3—C8	110.9(2)	112.51	110.97
C8—N2—N1	118.6(2)	120.88	121.01
N2—N1—C7	117.2(2)	119.11	118.42
N1—C7—C1	121.5(3)	121.52	122.13
C1—C6—O1	121.8(2)	121.99	122.55
C11—C12—C13	89.2(3)	88.94	88.86
C13—C14—C11	89.2(3)	89.27	89.16
C14—C11—C12	88.8(2)	88.85	88.65
C12—C13—C14	88.1(2)	88.06	87.89
RMSE ^a		1.32	0.99
Max. difference ^a		2.28	2.41
<i>Torsion angles (°)</i>			
N2—N1—C7—C1	179.1(2)	179.61	179.38
C7—N1—N2—C8	179.3(2)	177.96	177.34
N1—N2—C8—N3	-176.9(2)	-179.37	-179.20
C7—C1—C6—O1	0.9(4)	0.16	0.19
C9—N3—C8—N2	178.8(2)	179.51	179.67
N1—N2—C8—S1	3.2(4)	0.45	0.75
RMSE ^a		1.82	1.80
Max. difference ^a		2.77	2.47

^a RMSE and maximum differences between the bond lengths and the bond angles computed by the theoretical method and those obtained from X-ray diffraction.

3.2. Optimized structures

In order to verify the accuracy of used theoretical model the investigated molecule is fully optimized in the gas phase and optimized geometry compared with experimental geometry. According

**Fig. 3.** The experimental FT-IR spectrum of the title compound.

to X-ray study dihedral angles between the A, B, C planes are calculated as 2.52° (A/B), 76.69° (A/C), 76.75° (B/C) for 6-31G basis set and 3.19° (A/B) 74.24° (A/C), 74.24° (B/C) for 6-31G(d,p) basis set. The dihedral angle between the C14/C13/C12 and the C12/C11/C14 planes (puckering of the cyclobutane ring) is calculated as 23.46° for 6-31G basis set and 24.79° for 6-31G(d,p) basis set. Selected bond lengths, bond angles and torsion angles of optimized geometry are listed in Table 3 with experimental ones.

As can be seen in Table 3 most of the calculated bond lengths are slightly longer than the experimental ones except N1—N2 and O1—C6 which are shorter. The largest difference between experimental and calculated bond length is 0.093 Å which is calculated with 6-31G basis set for S1—C10. The largest difference between experimental and calculated bond angle is 2.41° which is calculated with B3LYP/6-31G(d,p) for C8—N2—N1. It is well known that for an accurate description at least double zeta quality basis augmented with a set of polarization functions set is needed. Therefore a somewhat better geometry description is expected with 6-31G(d,p) basis set. Using the root mean square (RMS) error for consideration it is found that the B3LYP/6-31G(d,p) calculation provide the lowest RMS value of 0.032 Å and 0.99° for bond lengths and bond angles respectively. Consequently the B3LYP calculation with 6-31G(d,p) basis set predicts the best geometry when compared the calculation with 6-31G basis set.

3.3. IR spectroscopy

FT-IR spectrum are obtained in KBr disks using a Mattson 1000 FT-IR spectrometer, and shown in Fig. 3. Based on optimized geometries harmonic vibrational frequencies were calculated by using same method and basis sets as. The calculated frequencies were not scaled. Frequency calculations at the same level of theory revealed no imaginary frequencies indicating that an optimal geometry at these levels of approximation was found for the title compound. By using Gauss View molecular visualization program [31], the vibrational band assignments have been made. The experimental and calculated frequencies are given in Table 4 with their assignments. It is well known that the calculated 'non-scale' harmonic frequencies could significantly overestimate experimental values due to lack of electron correlation, insufficient basis sets and anharmonicity and noted that the experimental results belong to solid phase and theoretical calculations belong to gaseous phase. Thus there is a reasonable agreement between experimental and calculated frequencies, except for the OH and NH stretching bands. The $\nu_{\text{str}}(\text{O—H})$ vibration of crystalline water is observed at 3563 cm^{-1} and is calculated 3755 cm^{-1} and 3857 cm^{-1} for 6-31G

Table 4
Comparison of the observed and calculated vibrational spectra (cm^{-1}) of the title compound.

Assignments	Experimental	DFT/B3LYP	
		6-31G	6-31G(d,p)
$\nu_{\text{asym-str}}$ (OH) water	3563	3755	3857
$\nu_{\text{sym-str}}$ (OH) water	–	3253	3528
ν_{str} (OH) phenol	3320	3215	3443
ν_{str} (CH) thiazole	3218	3323	3283
ν_{str} (NH) hydrazone	3159	3253	3254
ν_{str} (CH) aromatic	3070	3231	3210
$\nu_{\text{sym-str}}$ (CH) aromatic	3055	3222	3205
$\nu_{\text{asym-str}}$ (CH) aromatic	3022	3200	3171
$\nu_{\text{asym-str}}$ (CH_2)	2945	3135	3121
$\nu_{\text{asym-str}}$ (CH_3)	2930	3111	3108
$\nu_{\text{sym-str}}$ (CH_2)	2858	3073	3063
$\nu_{\text{sym-str}}$ (CH_3)	2848	3035	3036
ν_{sci} (OH) water	–	1642	1689
ν_{str} (C=N) hydrazone + ν_{bend} (NH)	1654	1697	1671
ν_{str} (C=N) thiazole + ν_{bend} (NH) hydrazone	1619	1667	1640
ν_{str} (CC) aromatic	1596	1638	1637
ν_{str} (C=C) thiazole	1564	1601	1587
ν_{sci} (CH_2)	1444	1512	1507
ν_{bend} (OH) phenol	1420	1519	1434
ν_{sci} (CH_3)	1346	1453	1419
ν_{wag} (CH_2)	1298	1288	1331
	1221	1297	1311
ν_{bend} (CH) aromatic	1168	1222	1187
ν_{twist} (CH_2)	1105	1173	1162
$\nu_{\text{bend-out of plane}}$ (CH) aromatic	859	879	860
ν_{rock} (CH_2)	789	875	852
$\nu_{\text{bend-out of plane}}$ (OH) phenol	762	772	759
$\nu_{\text{bend-out of plane}}$ (NH)	720	830	783
$\nu_{\text{bend-out of plane}}$ (CC)	700	797	761
ν_{bend} (C–S–C)	658	–	–

Vibrational modes: str; stretching, bend; bending, sci; scissoring, rock; rocking, wag; wagging, twist; twisting, sym; symmetric, asym; asymmetric.

and 6-31G(d,p) respectively. The band observed at 3320 cm^{-1} is attributed to the absorption of the $\nu_{\text{str}}(\text{O–H})$ vibration of phenol which is calculated 3215 cm^{-1} and 3443 cm^{-1} for 6-31G and 6-31G(d,p) respectively. The NH stretching band is observed at 3159 cm^{-1} which is calculated 3253 cm^{-1} and 3254 cm^{-1} for 6-31G and 6-31G(d,p) respectively. Such differences between experimental and calculated frequencies for $\nu_{\text{str}}(\text{O–H})$ and $\nu_{\text{str}}(\text{N–H})$ bands could be expected for such modes in a medium strong hydrogen bond [40]. Since our main interest of IR study is the characterization of intramolecular and intermolecular hydrogen bonds so no elaborate normal mode analysis was performed and only the approximate description of selected modes is given in Table 4.

3.4. Molecular electrostatic potential

The molecular electrostatic potential (MEP) is related to the electronic density and is a very useful descriptor for determining sites of chemical reactivity of the molecule for electrophilic attack and nucleophilic reactions as well as hydrogen-bonding interactions [41–43]. To predict reactive sites for electrophilic and nucleophilic attack for the title molecule, MEP was calculated at the B3LYP/6-31G(d,p) optimized geometry. The negative (red) regions of MEP were related to electrophilic reactivity and the positive (blue¹) regions to nucleophilic reactivity shown in Fig. 4. It can be seen from Fig. 4 there are two possible sites on the title compound for electrophilic attack with a maximum value of -0.0641 a.u. . However, positive (blue) regions are localized on

¹ For interpretation of color in Figs. 1, 2, 4, 5 and 8, the reader is referred to the web version of this article.

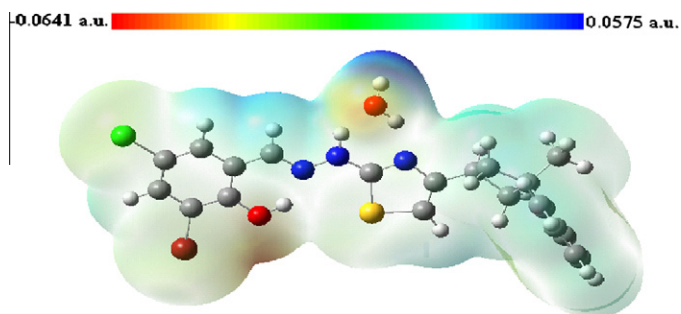


Fig. 4. Molecular electrostatic potential map (in a.u.) of the title compound computed with the B3LYP/6-31G(d,p) level.

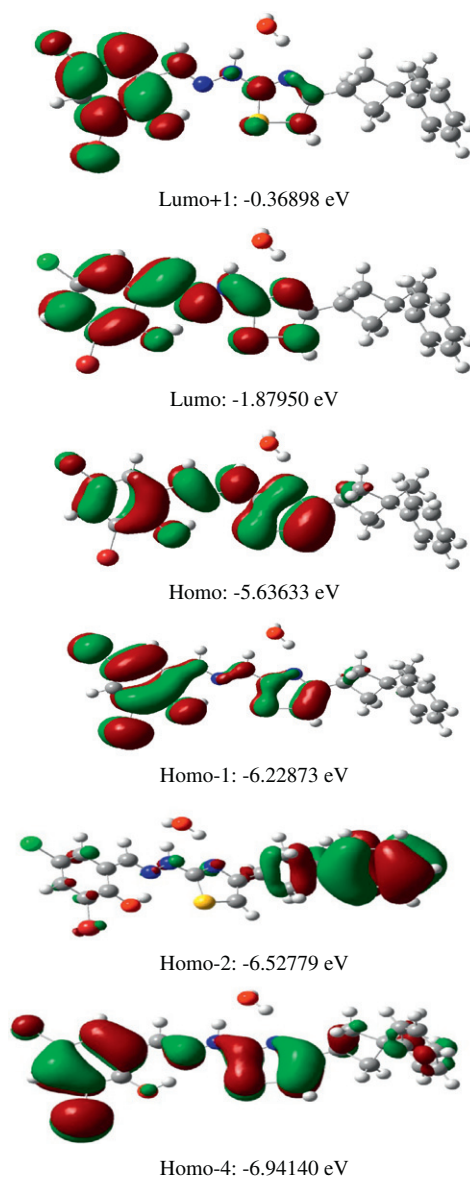


Fig. 5. Molecular orbital surfaces and energy levels given in parentheses for the HOMO-4, HOMO-2, HOMO-1, HOMO, LUMO, LUMO + 1 of the title compound computed with the B3LYP/6-31G(d,p) level.

hydrogen atoms of water molecule and C7 atom with a maximum value of 0.0575 a.u. . These results provide information concerning the region where the compound can interact intermolecularly.

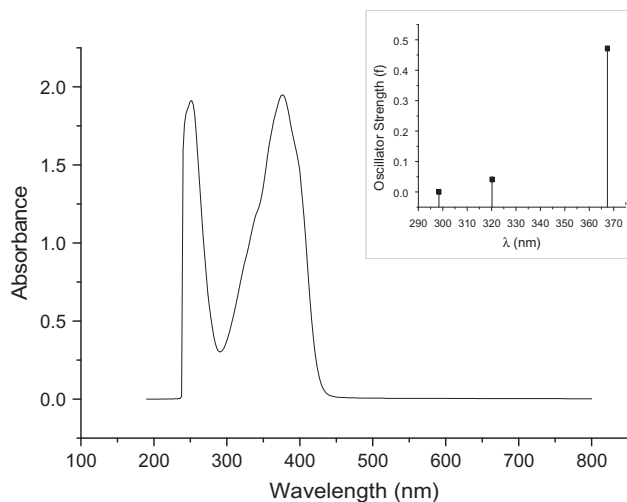


Fig. 6. The experimental absorption spectrum of the title compound in CHCl_3 solution. Inset: calculated absorption spectra of title compound. The excited states are shown as vertical bars with high equal to oscillator strength.

3.5. Frontier molecular orbital analysis and absorption spectra

Analyses of frontier molecular orbital provide helpful information for studies on electrical and optical properties as well as in UV–Vis spectrum and chemical reactions [44]. Fig. 5 shows surface and energy levels of the HOMO-4, HOMO-2, HOMO-1, HOMO, LUMO and LUMO + 1 orbitals which are computed at the B3LYP/6-31G(d,p) for the title compound. The calculations indicate that the compound has 126 occupied MOs. From Fig. 5 both the highest occupied molecular orbitals (HOMOs) and the lowest unoccupied molecular orbitals (LUMOs) mainly delocalized on the thiazole and phenol rings connected with hydrazone linkage. The HOMOs are mostly π -bonding type orbitals and the LUMOs are π -antibonding type orbitals.

The absorption spectrum of the title compound was recorded in CHCl_3 at room temperature and theoretical absorption spectrum is predicted by using TD-DFT method based on B3LYP/6-31G(d,p) level optimized structure. A comparison of calculated (vertical excitations) and experimental electronic spectrum is reported in Fig. 6 and all of the data are listed in Table 5. The visible absorption spectrum of the title compound appears as highly intense absorption bands at 376 nm and 252 nm which are mainly due to π - π^* transition. As seen from Fig. 6 three bands appeared in the calculated spectrum having some differences compared with the corresponding experimental ones. The reasons for the discrepancy between the experimental values and theoretical predictions may be as follows: TD-DFT approach is based on the random-phase approximation method (RPA) [45–47] which provides an alternative to computationally demanding multireference configuration interaction methods in the study of excited states. TD-DFT calculations

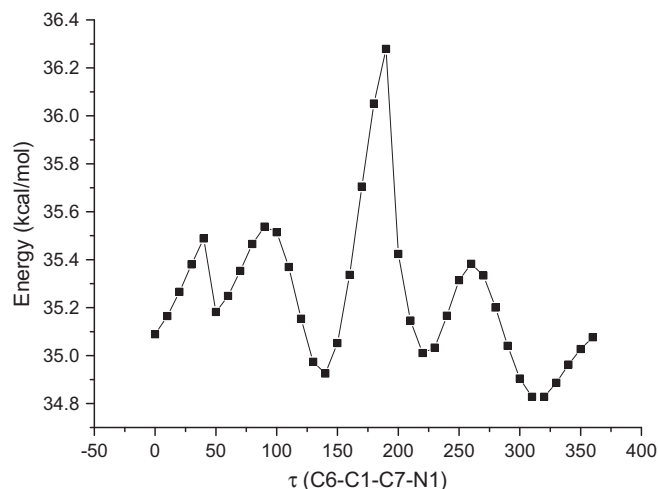


Fig. 7. Energy profile of the optimized counterpart of the title compound for the rotation about $\tau(\text{C6-C1-C7-N1})$ torsion angle.

do not evaluate the spin-orbit splitting; the values are averaged. Here, in this paper the objective is to evaluate the electronic structure by direct electronic excitations and only singlet-singlet transitions considered. In addition the role of solvent effect of solution is not included in the theoretical calculation.

3.6. Conformational analysis

In order to determine the preferential position of phenol ring with respect to hydrazone fragment a preliminary search of low energy structures was performed using AM1 computations as a function of the selected degrees of torsional freedom τ (C6–C1–C7–N1). The calculated energy profile with respect to rotations about the selected torsion angle $\tau(\text{C6-C1-C7-N1})$ is given in Fig. 7 and the optimized geometries of the most favorable and unfavorable conformations are illustrated in Fig. 8a and b respectively. The respective value of the selected degree of torsion angle $\tau(\text{C6-C1-C7-N1})$ is $0.85(40)^\circ$ in X-ray structure, whereas the corresponding value in optimized geometry is -0.36° for B3LYP/6-31G and -0.57° for B3LYP/6-31G(d,p). As can be seen from Fig. 7 the minimum energy domain is located at 310° having energy of $34.827 \text{ kcal mol}^{-1}$, the maximum energy is also located at 190° having energy of $36.279 \text{ kcal mol}^{-1}$. Energy difference between the most favorable and unfavorable conformer, which arises from rotational potential barrier calculated with respect to the selected torsion angle, is calculated as $1.452 \text{ kcal mol}^{-1}$ when both selected degrees of torsion angle are considered.

The molecular energy can be divided into bonded and non-bonded contributions. The bonded energy is considered to be independent of torsional angle changes and therefore vanished when relative conformer energies are calculated. The non-bonded energy

Table 5
Experimental and theoretical electronic absorption spectra values.

Excitation	Electronic transition	Oscillator strength (<i>f</i>)	λ_{theo} (nm)	λ_{exp} (nm)
1	126(HOMO) → 127(LUMO)	0.4713	367.42	376
2	122(HOMO-4) → 128(LUMO + 1)	0.0410	320.19	
	124(HOMO-2) → 127(LUMO)			
	125(HOMO-1) → 127(LUMO)			
	126(HOMO) → 128(LUMO + 1)			
3	124(HOMO-2) → 127(LUMO)	0.0001	298.41	252
	125(HOMO-1) → 127(LUMO)			

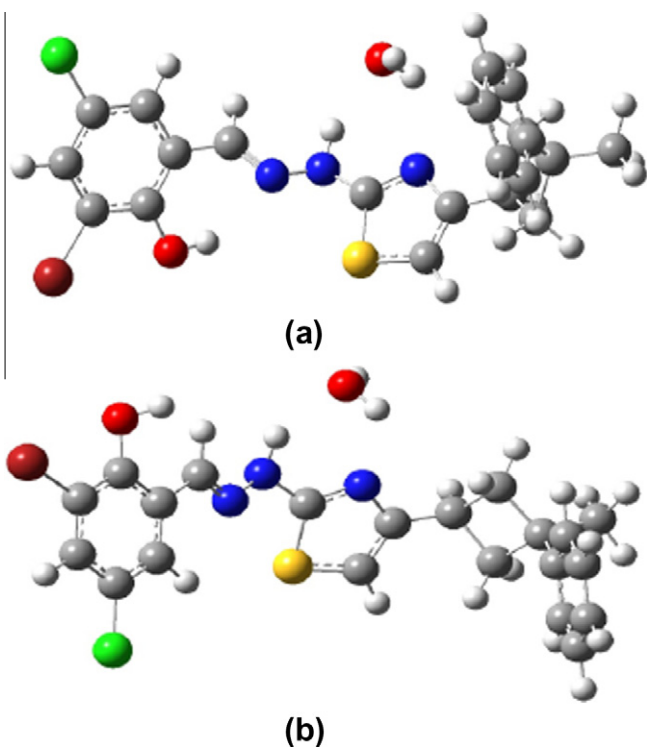


Fig. 8. The optimized geometries of the most favorable and unfavorable conformations for the selected torsion angle (a) the most favorable conformation and (b) unfavorable conformation.

is further separated into torsional steric and electrostatic terms [48]. It is clearly shown from Fig. 8a and b that the principal difference between the most favorable and unfavorable conformers for selected torsion angle is proceed the orientation of hydrogen atom of —OH moiety with respect to —CH group of hydrazone. Owing to the fact that the title compound contains an $\text{O—H} \cdots \text{N}$ intramolecular hydrogen bond, the computational results allow us to predict the most stable conformer is principally determined by the non-bonded torsional energy and electrostatic energy terms affected by packing of the molecules.

4. Conclusions

The synthesis, FT-IR and UV–Vis, crystal and molecular structure determined by single-crystal X-ray diffraction as well as density functional theory calculations of 2-bromo-4-chloro-6-[[4-(3-methyl-3-phenyl-cyclobutyl)-thiazol-2-yl]-hydrazonomethyl]-phenol is reported. The X-ray structure is slightly different from its optimized counterparts. Crystal structure is stabilized by $\text{N—H} \cdots \text{O}$, $\text{O—H} \cdots \text{O}$ and $\text{C—H} \cdots \text{O}$ type hydrogen bonds. These hydrogen bonds supply leading contribution to the stability and are presumably responsible for the inconsistencies between the X-ray and optimized structures of title compound. The geometric parameters which were using method with 6-31G(d,p) basis set are in good agreement with the experimental ones. The IR spectrum supported by DFT calculations was particularly devoted to the manifestations of hydrogen bonding in the $\nu_{\text{str}}(\text{N—H})$ and $\nu_{\text{str}}(\text{O—H})$ vibrations. As a result, all of these calculations will be provide helpful information to further studies on the title compound.

Supplementary material

CCDC 777381 contains the supplementary crystallographic data for this paper. These data can be obtained free of charge at www.ccdc.cam.ac.uk/conts/retrieving.html [or from the Cam-

bridge Crystallographic Data Centre (CCDC), 12 Union Road, Cambridge CB2 1EZ, UK; fax: +44 (0)1223 336033; email: deposit@ccdc.cam.ac.uk].

References

- [1] S.R. Sheeja, N.A. Mangalam, M.R.P. Kurup, Y.S. Marry, K. Raju, H.T. Varghese, C.Y. Panicker, *J. Mol. Struct.* 973 (2010) 36.
- [2] N. Terzioglu, A. Gurosy, *Eur. J. Med. Chem.* 38 (2003) 781.
- [3] M.T. Cocco, C. Congiu, V. Lilliu, V. Onnis, *Bioorg. Med. Chem.* 14 (2006) 366.
- [4] J. Easmon, G. Puerstinger, T. Roth, H.H. Fiebig, M. Jenny, W. Jaeger, G. Heinisch, *J. Hofmann, Int. J. Cancer* 94 (2001) 89.
- [5] P. Vicini, F. Zani, P. Cozzini, I. Doytchinova, *Eur. J. Med. Chem.* 37 (2002) 553.
- [6] J. Patole, U. Sandbhor, S. Padhye, D.N. Deobagkar, C.E. Anson, A. Powell, *Bioorg. Med. Chem. Lett.* 13 (2003) 51.
- [7] A. Walcourt, M. Loyevsky, D.B. Lovejoy, V.R. Gordeuk, D.R. Richardson, *Int. J. Biochem. Cell Biol.* 36 (2004) 401.
- [8] F. Kratz, U. Beyer, T. Roth, N. Tarasova, P. Collery, F. Lechenault, A. Cazabat, P. Schumacher, C. Unger, U. Falken, *J. Pharm. Sci.* 87 (1998) 338.
- [9] S. Sivaramaiah, P.R. Reddy, *J. Anal. Chem.* 60 (2005) 828.
- [10] S.H. Babu, K. Suvardhan, K.S. Kumar, K.M. Reddy, D. Rekha, P. Chiranjeevi, *J. Hazard. Mater.* 120 (2005) 213.
- [11] S.A. Berger, *Microchem. J.* 47 (1993) 317.
- [12] A.A. El-Emam, F.F. Belal, M.A. Moustafa, S.M. El-Ashry, D.T. El-Sherbiny, S.H. Hansen, *II Farmaco.* 58 (2003) 1179.
- [13] M.G. El-Meligy, S. El-Rafie, K.M. Abu-Zied, *Desalination* 173 (2005) 33.
- [14] M. Bakir, I. Hassan, T. Johnson, O. Brown, O. Green, C. Gyles, M.D. Coley, *J. Mol. Struct.* 688 (2004) 213.
- [15] X. Ge, I. Wendler, P. Schramel, A. Kettrup, *React. Funct. Polym.* 61 (2004) 1.
- [16] A.V. Xavier (Ed.), *Frontiers in Bioinorganic Chemistry*, VCH, Portugal, 1985.
- [17] H. Tezcan, T. Tunç, E. Şahin, R. Yagbasan, *Anal. Sci.* 20 (2004) 137.
- [18] A. Townshend, R.A. Wheatly, *Analyst* 123 (1998) 1041.
- [19] I. Pozdnyakova, P.W. Stafshede, *Biochemistry* 40 (2001) 13728.
- [20] U. Kuehn, S. Warzeska, H. Pritzkow, R.J. Kramer, *Am. Chem. Soc.* 123 (2001) 8125.
- [21] K.D. Karlin, J. Zubieta, *Biochemistry Chemical and Inorganic Perspectives*, Adenine Press, Guilderland, New York, 1983.
- [22] M.J. Wojcik, J. Kwiedacz, M. Boczar, L. Boda, Y. Ozaki, *Chem. Phys.* 372 (2010) 81.
- [23] G.M. Sheldrick, *SHELXS-97 and SHELXL-97; Program for Solution of Crystal Structures*, Univ. Gottingen, Germany, 1997.
- [24] L.J. Farrugia, *J. Appl. Crystallogr.* 30 (1999) 837.
- [25] G.M. Sheldrick, *SHELXS-97 and SHELXL-97; Program for Refinement of Crystal Structures*, Univ. Gottingen, Germany, 1997.
- [26] Stoe & Cie, *X-AREA Version 1.18 and X-RED32 (Version 1.04)*, Stoe & Cie, Darmstadt, Germany, 2002.
- [27] L.J. Farrugia, *J. Appl. Crystallogr.* 30 (1997) 565.
- [28] M.J. Frisch, G.W. Trucks, H.B. Schlegel, G.E. Scuseria, M.A. Robb, J.R. Cheeseman, J.A. Montgomery, T. Vreven, K.N. Kudin, J.C. Burant, J.M. Millam, S.S. Iyengar, J. Tomasi, V. Barone, B. Mennucci, M. Cossi, G. Scalmani, N. Rega, G.A. Petersson, H. Nakatsuji, M. Hada, M. Ehara, K. Toyota, R. Fukuda, J. Hasegawa, M. Ishida, T. Nakajima, Y. Honda, O. Kitao, H. Nakai, M. Klene, X. Li, J.E. Knox, H.P. Hratchian, J.B. Cross, C. Adamo, J. Jaramillo, R. Gomperts, R.E. Stratmann, O. Yazyev, A.J. Austin, R. Cammi, C. Pomelli, J.W. Ochterski, P.Y. Ayala, K. Morokuma, G.A. Voth, P. Salvador, J.J. Dannenberg, V.G. Zakrzewski, S. Dapprich, A.D. Daniels, M.C. Strain, O. Farkas, D.K. Malick, A.D. Rabuck, K. Raghavachari, J.B. Foresman, J.V. Ortiz, Q. Cui, A.G. Baboul, S. Clifford, J. Cioslowski, B.B. Stefanov, G. Liu, A. Liashenko, P. Piskorz, I. Komaromi, R. Martin, D.J. Fox, T. Keith, M.A. Al-Laham, C.Y. Peng, A. Nanayakkara, M. Challacombe, P.M.W. Gill, B. Johnson, W. Chen, M.W. Wong, C. Gonzalez, J.A. Pople, *Gaussian 03: IA32WG03RevC 02 12-Jun-2004*, Gaussian, Inc., Wallingford, CT, 2004.
- [29] C. Lee, W. Yang, R.G. Parr, *Phys. Rev. B* 37 (1988) 785.
- [30] A.D. Becke, *J. Chem. Phys.* 98 (1993) 5648.
- [31] R. Dennington II, T. Keith, J. Millam, *GaussView, Version 4.1.2*, Semichem Inc. Shawnee Mission, KS, 2007.
- [32] D.C. Swenson, M. Yamamoto, D.J. Burton, *Acta Cryst.* C53 (1997) 1445.
- [33] F. Güntepe, H. Saraçoğlu, N. Çalışkan, Ç. Yüseketepe, A. Çukurovalı, *J. Struct. Chem.* 52 (2011) 596.
- [34] F.H. Allen, *Acta Crystallogr.* B40 (1984) 64.
- [35] N. Özdemir, M. Dinçer, A. Çukurovalı, *J. Mol. Model.* 16 (2010) 291.
- [36] N. Kohata, T. Fukuyama, K. Kuchitsu, *J. Phys. Chem.* 86 (1982) 602.
- [37] V.A. Naumov, O.A. Litvinov, H.J. Geise, J. Dillen, *J. Mol. Struct.* 99 (1983) 303.
- [38] G. Pavlovic, L. Racane, H. Cicak, V. Tralic-Kulenovic, *Dyes Pigments* 83 (2009) 354.
- [39] J. Bernstein, R.E. Davis, L. Shimoni, N.L. Chang, *Angew. Chem. Int. Ed. Eng.* 34 (1995) 1555.
- [40] T. Steiner, *Angew. Chem. Int. Ed.* 41 (2002) 48.
- [41] E. Scrocco, J. Tomasi, *Adv. Quant. Chem.* 11 (1979) 115.
- [42] F.J. Luque, J.M. Lopez, M. Orozco, *Theor. Chem. Acc.* 103 (2000) 343.
- [43] N. Okulik, A.H. Jubert, *Internet Electron. J. Mol. Des.* 4 (2005) 17.
- [44] I. Fleming, *Frontier Orbitals and Organic Chemical Reactions*, Wiley, London, 1976.
- [45] J. Song, P.S. Zhao, W.G. Zhang, *Bull. Korean Chem. Soc.* 31 (2010) 1875.
- [46] M. Fernando, O.A. Claudio, *Int. J. Quant. Chem.* 103 (2005) 34.
- [47] L. Olsenand, P. Jorgensen, in: *Modern Electronic Structure Theory*, World Science, 2, River Edge, NJ, 1995.